

**APPLICATIONS OF THE WAVELET TRANSFORM IN AFM DATA ANALYSIS<sup>1</sup>****P. Klapetek<sup>\*,2</sup>, I. Ohlídal<sup>†</sup>***\* Czech Metrology Institute, Okružní 31, 638 00 Brno, Czech Republic,**† Department of Physical Electronics, Faculty of Science, Masaryk University, Kotlářská 2, 611 37 Brno, Czech Republic,*

Received 11 February 2005, accepted 23 February 2005

In this article the possibilities of the wavelet transform use within atomic force microscopy data processing are presented. Both discrete and continuous wavelet transform is used for different processing and analytical purposes including denoising, AFM scan error detection, background removal and multifractal analysis. It is shown that the use of wavelet transform can be very effective within AFM data analysis, namely for highly irregular data.

PACS: 68.37.Ps

**1 Introduction**

In the last twenty years wavelet transform became important tool for data processing. Wavelet transform is a transform similar to well-known Fourier transform. Fourier transform decomposes the signal into sines and cosines - i. e. to the functions localized in frequency domain. On the contrary, wavelet transform uses merit functions that are localized in both the real space and frequency domain. This enables us to determine locally spatial frequencies present in data.

There are many applications of the two-dimensional wavelet transform, namely in the field of digital image processing as interpolation [1], denoising [2, 3] and fractal analysis [4]. There are also a few papers in the literature dealing with applications of the wavelet transform directly in AFM data analysis [5].

In this article we present some algorithms known from the digital image processing, applied and modified for AFM data analysis. We show that in many cases the wavelet transform approach can be very effective for AFM data processing.

We use both continuous and discrete wavelet transform for different analytical purposes. Discrete wavelet transform applications include denoising, AFM scan error detection and background subtraction. The continuous wavelet transform is employed for background subtraction and for multifractal analysis of the scaling properties of randomly rough surfaces.

---

<sup>1</sup>Presented at SSSI-IV (Solid State Surfaces and Interfaces IV) Conference, Smolenice, Slovakia, 8–11 Nov. 2004.<sup>2</sup>E-mail address: klapetek@physics.muni.cz

## 2 Wavelet transform for AFM data analysis

In general, the continuous wavelet transform in one dimension is defined as

$$W(a, b) = \frac{1}{\sqrt{|a|}} \int_{-\infty}^{\infty} f(x) \psi^* \left( \frac{x-b}{a} \right) dx, \quad (1)$$

where parameter  $a$  controls scale of the wavelet (its magnification) and parameter  $b$  controls its shift along the  $x$  axis. Using wavelet transform we decompose the original signal  $f(x)$  into a set of differently shifted and scaled basis functions called wavelets  $\psi$ . The asterisk denotes complex conjugate.

As it is seen, the relation (1) describes an infinite set of various transforms, depending on the merit function used for computation. Therefore, we can find very large amount of different space-frequency analysis methods called as wavelet transform in the literature. Basically, we can divide the most widely used merit functions from the point of their orthogonality:

**Orthogonal wavelets** (e. g. Haar wavelet, Daubechies wavelets) that are orthogonal to their own dilations and translations and that are used to develop the non-redundant discrete wavelet transform. The discrete wavelets can be shifted and scaled only in discrete steps. When we denote the discrete wavelet as  $\psi_{a,b}$  scaling factor as  $a$  and shift factor as  $b$  we can express the orthogonality as follows

$$\int_{-\infty}^{\infty} \psi_{j,k} \psi_{m,n}^* = 0, \quad (2)$$

if  $j \neq m$  and  $k \neq n$ .

**Non-orthogonal wavelets** (e. g. Morlet wavelet, Mexican hat wavelet) are used to develop the redundant continuous wavelet transform.

As an example, the orthogonal Daubechies wavelet and non-orthogonal Morlet wavelet is plotted in Fig. 1. There are more wavelet types and transforms, however the two presented here are most widely used and can serve as examples of two main types of the wavelet transform: redundant and non-redundant ones.

The **discrete wavelet transform** (DWT) returns a data vector of the same length as the input data length is. This corresponds to the fact that it decomposes into a set of wavelets (functions) that are orthogonal to its translations and scaling. Therefore, using limited number of given scales and translation for wavelet transform computation we decompose a signal to the same number of the wavelet coefficients comparing to number of signal data points. Usually, in the discrete wavelet transform result many data points are almost zero. Such a wavelet spectrum is therefore very good for signal processing and compression, for example, as we get no redundant information as a result of the transform.

In contrary, the **continuous wavelet transform** returns an array one dimension larger than the dimension of the input data is. For a 1D series we therefore obtain an image of the space-frequency plane (often called wavelet scalogram, wavelet spectrum or wavelet dynamic spectrum). We can easily see the signal frequencies evolution along the series and compare the wavelet spectrum with other series wavelet spectra. As here the non-orthogonal set of wavelets

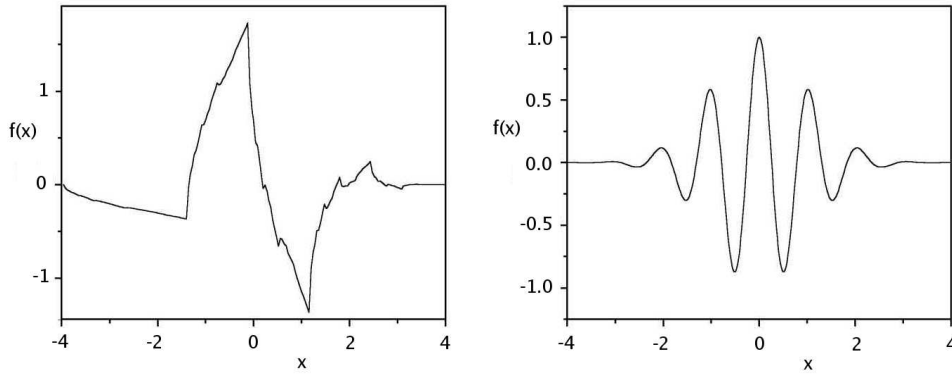


Fig. 1. Daubechies 20 wavelet (left) and real part of the Morlet wavelet (right).

is used, data are highly correlated and big redundancy can be seen in the result. This usually helps to see the results in a more humane form comparing to discrete wavelet transform results. Moreover, we can compute the continuous wavelet transform spectrum for any set of scales and translations. This property is useful namely for data filtering purposes and for determining data scaling properties (e. g. using the fractal analysis). For details of the wavelet transform theory see e. g. Ref. [6].

Within AFM data analysis, we work with two-dimensional (2D) discrete and continuous wavelet transforms. In Figure 2 an AFM image and its the 2D DWT decomposition is presented. We can see that at each scale we obtain three subimages corresponding to horizontal, diagonal and vertical details. Note that there are the wavelet coefficients obtained directly by 2D DWT plotted in the Figure 2. We will use these wavelet coefficients at different levels of decomposition for denoising the AFM data, scanning defect identification and background removal.

Furthermore, we will use two-dimensional continuous wavelet transform (2D CWT) for the background removal and multifractal analysis of randomly rough surfaces.

## 2.1 Denoising

Atomic force microscope is designed for very large signal to noise ratio while measuring at micrometer scale. However, the noise influence becomes important while measuring very fine structures. Moreover, within some other AFM-related analytical methods (e.g. magnetic force microscopy or near-field scanning optical microscopy) the signal to noise ratio can be much smaller. Thus the denoising procedure needs to be often applied to the AFM data.

For data denoising we used 2D DWT in the following manner:

1. We compute direct 2D DWT of the AFM data.
2. We threshold the wavelet coefficients in each scale, i. e. we remove or lower the coefficients that are smaller than predefined threshold value.

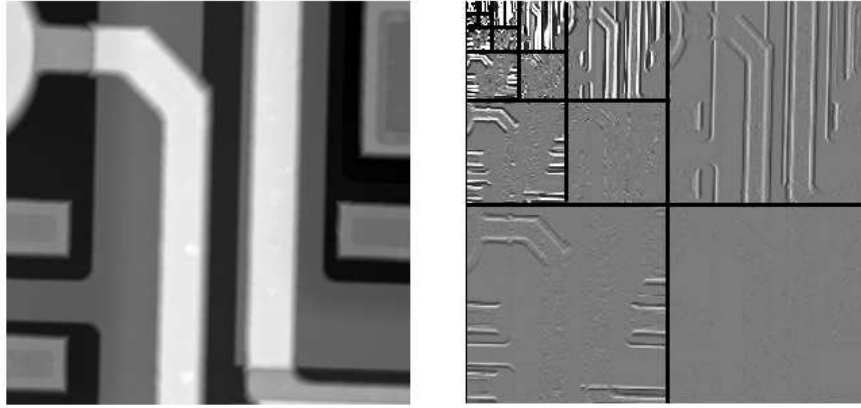


Fig. 2. AFM image of the microchip surface (left) and its discrete wavelet transform (right).

3. We compute inverse 2D DWT of the processed wavelets coefficients.

The main problem is determination of the threshold value for different scales of the wavelet coefficients. For AFM data processing we use two simple methods — scale adaptive thresholding [2] and scale and space adaptive thresholding [3]. For threshold determination within both the methods we first determine the noise variance guess given by

$$\hat{\sigma} = \frac{\text{Median}|Y_{ij}|}{0.6745} \quad (3)$$

where  $Y_{ij}$  corresponds to all the coefficients of the highest scale subband of the decomposition (where most of the noise is assumed to be present). Alternatively, the noise variance can be obtained in an independent way, for example from the AFM signal variance while not scanning (i. e. the free oscillations of the AFM probe). For each subband (for scale adaptive thresholding) or for each pixel neighbourhood within subband (for scale and space adaptive thresholding) the variance is computed as

$$\hat{\sigma}_Y^2 = \frac{1}{n^2} \sum_{i,j=1}^n Y_{ij}^2. \quad (4)$$

Threshold value is finally computed as

$$T(\hat{\sigma}_X) = \hat{\sigma}^2 / \hat{\sigma}_X, \quad (5)$$

where  $\hat{\sigma}_X = \sqrt{\max(\hat{\sigma}_Y^2 - \hat{\sigma}^2, 0)}$ . When threshold for given scale is known, we can remove all the coefficients smaller than threshold value (hard thresholding) or we can lower the absolute value of these coefficients by threshold value (soft thresholding).

In Figure 3 the noisy and denoised AFM image of mica is presented. It corresponds to atomic resolution topography measured in air by commercial AFM (Veeco Explorer). We can

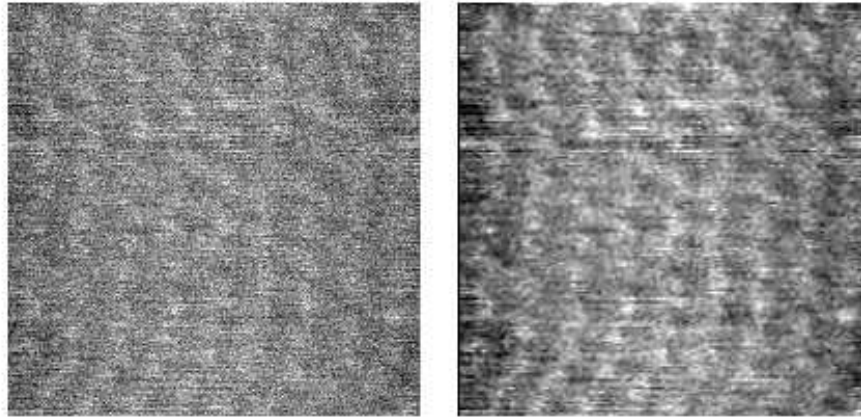


Fig. 3. AFM image of the atomic resolution on mica before (left) and after (right) scale and space adaptive threshold denoising.

see that the periodic structure is enhanced by means of denoising. However, it should be noted that there was no a priori information about the spatial frequencies expected in the data used for denoising. This is the main difference from Fourier transform denoising that is often used for atomic resolution images enhancement. Other important property of the DWT denoising is that it is local and therefore it does not cause unwanted blurring of the data in case that edges or fine structures are present at data.

## 2.2 Defect identification

As it was seen in Figure 2, there is a separated information about wavelet coefficients corresponding to different directions in the DWT decomposition. In this section we will use this information for local anisotropy detection, in particular for scanning defects localization.

The most common defect within AFM measurements is the weak closed loop performance. In case that the closed loop parameters are not set correctly (for example while scanning some unexpected high surface irregularities) we can observe a kind of stripes in the fast scanning axis direction (here in the X-direction). From practical point of view, sometimes it can be very hard to prevent these artefacts completely (for example for surfaces polluted by dust or for charged surfaces) and these artefacts must be corrected after scanning.

A simple detection of stripes based on horizontal/vertical coefficient ratio at different levels was performed. When a value of this ratio larger than predefined threshold (determined experimentally) was found, we have marked the image point and its closest neighbourhood in given direction as stripe. As the wavelet coefficients at each decomposition level represent certain wavelet scale we marked different neighbourhood size for points found in different decomposition levels.

In Figure 4 the AFM image of ZnSe epitaxial thin film surface with clearly seen stripes is presented. The result of stripes identification by means of the wavelet method is also presented.

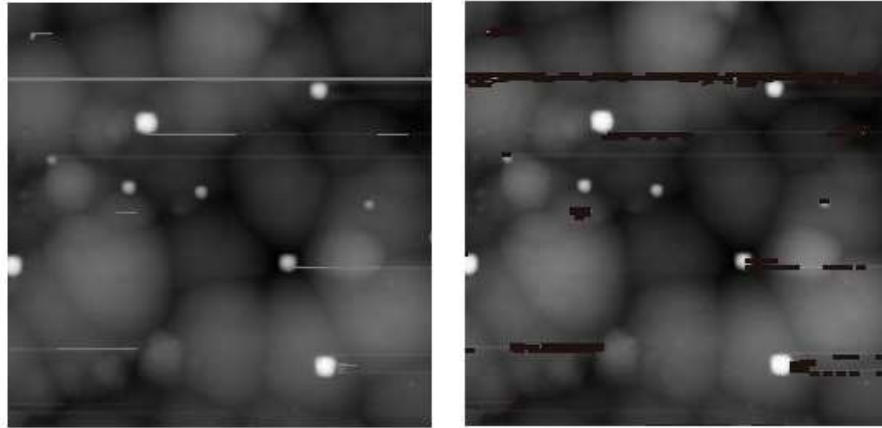


Fig. 4. AFM image of ZnSe thin film surface containing stripes (left) and same image with stripes marked by black colour (right)

We can see that the algorithm found the stripes very well. In the other hand it did not mark the particles not contaminated with stripes. Therefore, it can be used for AFM scan errors detection effectively. After marking all the stripes we can eliminate them using some interpolation algorithm.

### 3 Background subtraction

We can use both the DWT decomposition and CWT for separation of the different surface irregularities levels. In engineering applications this corresponds to “roughness”, “waviness” and “form” determination. This separation can be also done by means of Fourier transform methods. However, for highly irregular surfaces with different spatial frequencies present at different surface positions the Fourier transform method is not very effective.

If using CWT for background subtraction we choose certain wavelet scale and we compute 2D wavelet transform corresponding to that scale. The result is taken as background image. Foreground is determined by background subtraction from the original data usually — e. g. by subtracting the background data from the original data.

The DWT algorithm is very simple too: we take the AFM image and decompose it using 2D DWT. We choose some wavelet coefficients and use them for background subtraction (we compute inverse 2D DWT using only these coefficients). Then, we use the rest of wavelet coefficients to determine foreground image in the same way.

In Figure 5 an AFM image of hair is presented. We can see that there is a hair texture seen on the top. However, the raw image could be hardly used for texture analysis as the background geometry (cylinder) would corrupt the results strongly. In Figure 5 the results of the wavelet background subtraction are presented too. We can see that the details (hair texture - right image) are well separated from the form (cylinder - middle image). For this background subtraction the

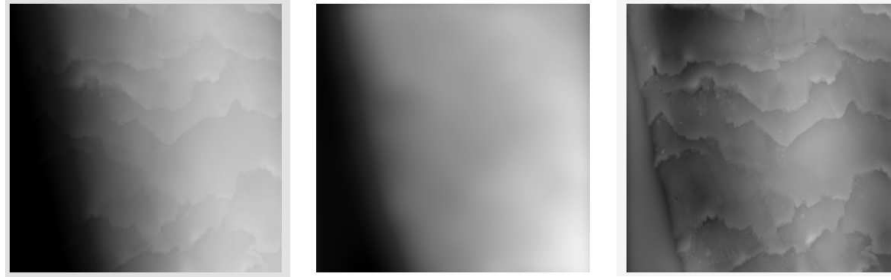


Fig. 5. AFM image of hair (left), extracted background (middle) and foreground (right).

2D CWT approach was used.

#### 4 Multifractal analysis

It can be shown, that the properties of the wavelet transform can be efficiently used for determining properties of singularities present in the data. We used the wavelet transform modulus maxima (WTMM) method developed by Arneodo [4] for multifractal analysis of AFM data. We will describe the method only very roughly here. For details, see Ref. [4]. The WTMM method is based on the following steps:

1. Wavelet transform modulus (module of the wavelet transform coefficients) is computed for different scales  $a$  of the wavelet.
2. Local maxima of wavelet transform modulus are found in the directions of wavelet modulus gradient. These maxima form connected chains.
3. Local maxima within connected chains are found. These points are used for further computation.
4. Points found in the previous step are interconnected through all scales  $a$  of the wavelet. This forms so called wavelet transform skeleton.
5. Scale adaptive partition function  $Z(q, a)$  is computed from the wavelet skeleton.

It is then assumed that the scale adaptive partition function has the following scaling properties:

$$Z(q, a) \sim a^{\tau(q)}. \quad (6)$$

where  $q$  is the order of scale adaptive partition function. The fractal properties of the surface can be then evaluated from the scaling exponents. For example, the fractal dimension is given by equation

$$D_f = \max(2, 1 - \tau(1)). \quad (7)$$

It can be shown that for fractional Brownian motion surface realization, that is often expected within randomly rough surface roughening models the scaling exponents are connected with the Hurst exponent  $H$  of the surface as

$$\tau(q) = qH - 2, \quad (8)$$

i.e. the  $\tau(q)$  function is a linear function of  $q$  with slope given by Hurst exponent. The linearity of function is thus a sign of monofractal properties of the surface. Moreover, from the dependences of  $\tau(q)$  it is possible to determine the Hurst exponent of the surface.

We used the method presented here for analysis of the fractal properties of rough GaAs surfaces created by thermal oxidation and dissolution of the oxide layer. Within the WTMM method we found that the fractal dimensions of GaAs surfaces are typically within the interval  $(2.4 \pm 0.1)$ . This result corresponds very well to the results obtained by traditional fractal analysis methods (e. g. cube counting). Moreover, we found the dependence of  $\tau(q)$  on  $q$  was not strictly linear for the real surfaces (see Fig. 6). This is in principal a sign of multifractal properties. Moreover, the nonlinearity of the corresponding functions can be also caused by the tip convolution effects.

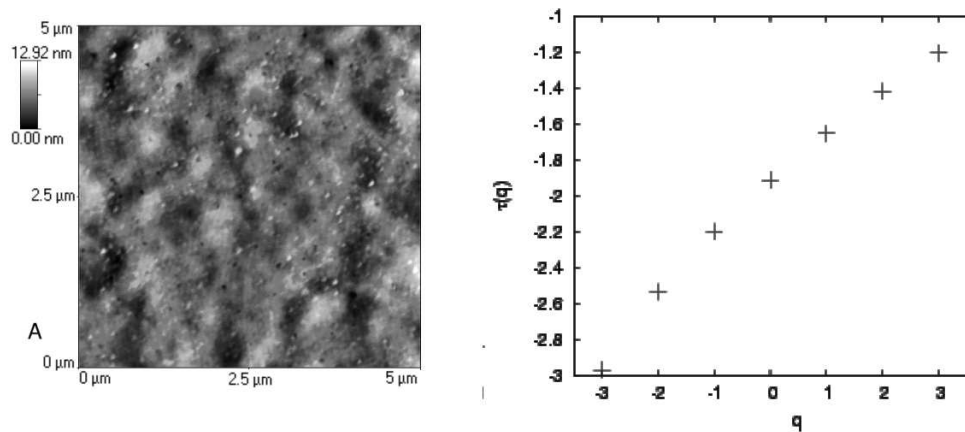


Fig. 6. AFM image of the GaAs surface (left) and  $\tau(q)$  (right) spectrum for this surface surfaces. The nonlinearity is a sign of multifractality.

## 5 Conclusion

In this article we have presented several wavelet-based methods that can be used for AFM data analysis purposes. We have found that both the discrete and continuous wavelet transform methods can be very effective in some typical processing applications as denoising and background subtraction. We have demonstrated possibilities of denoising and background subtraction on real samples.



The main advantage of the wavelet transform approach is the fact that the wavelet transform is a space-frequency decomposition method which localisation (width of the wavelets in real space) is controlled by single parameter (wavelet scale). We can therefore use the wavelet transform for detecting special features (e. g. stripes caused by not optimal closed loop settings) or evaluating local surface regularity (e. g. within multifractal analysis). The fact that discrete wavelet transform decomposes signal into horizontal, vertical and diagonal details is also very important from the practical point of view as the AFM instrument can introduce local anisotropy while measuring isotropic surface. We have found that the local anisotropy detection can be very useful for marking scanning defects that are sometimes observed at AFM data.

**Acknowledgement:** This work was supported by Ministry of Education of Czech Republic under contract MSM 143100003 and Ministry of Industry and Commerce of Czech Republic within the program TANDEM under contract No. FT-TA/094

#### References

- [1] O. G. Guleryuz: In: Data Compression Conference (DCC '02), Snao Bird, Utah, IEEE 2002.
- [2] S. G. Chang, B. Yu, M. Vetterli: IEEE Trans. Image Processing, **9** (2000) 1532
- [3] S. G. Chang, B. Yu, M. Vetterli: IEEE Trans. Image Processing, **9** (2000) 1522
- [4] A. Arnéodo, N. Decoster, S. G. Roux: Eur. Phys. J. B, **15** (2000) 567
- [5] B. Goolsby, Q. Chen, L. Udpa, Y. Fan, R. Samona, B. Bhooravan, F.M. Salam, D. H. Wang, V.M. Ayres: Journal of Nanoscience and Nanotechnology, **3** (2003) 347
- [6] A. Bultheel: Bull. Belg. Math. Soc.: **2** (1995) 1